

# Three-Dimensional Dielectric Characterization of Polymer Films

KAUSHAL S. PATEL,\* PAUL A. KOHL, SUE ANN BIDSTRUP-ALLEN

Georgia Institute of Technology, School of Chemical Engineering, Atlanta, Georgia 30332-0100

Received 15 May 2000; accepted 7 August 2000

**ABSTRACT:** Polymer films are widely used in electronic packaging applications due to their low dielectric constant and ease of fabrication. These films often exhibit anisotropic electrical and thermomechanical properties, due to orientation of polymer chains, which need to be evaluated for performance and reliability modeling of electronic packages. This article presents a dual-capacitor technique to measure the anisotropic dielectric permittivities of such films. Results are reported for *in situ* measurements for several spin-coated polymeric films, some of which exhibit different permittivities in the in-plane ( $x$  and  $y$ ) and the through-plane ( $z$ ) directions (transversely isotropic), and free-standing liquid crystalline Vectran films which exhibit orthotropic permittivities. © 2001 John Wiley & Sons, Inc. *J Appl Polym Sci* 80: 2328–2334, 2001

**Key words:** dielectric permittivity; anisotropy; dual-capacitor technique; liquid crystalline polymer; polyimide; benzocyclobutene; polynorbornene

## INTRODUCTION

Polymers dielectric films are widely used in microelectronics and electronic packaging applications, including circuit board substrates, passivation layers, and interlevel dielectrics in multichip modules<sup>1,2</sup> because they offer a lower dielectric constant and are more easily processed than are inorganic dielectrics. These films can display anisotropic properties as a result of chain orientation within the film, which needs to be measured for use in design and electrical performance modeling.

Polymer dielectrics are used as deposited films and free-standing films. Deposited polymer films can be coated onto a substrate from solution by spin-coating, spraying, or extrusion coating. After

deposition, the films are cured at an elevated temperature to remove the solvent and carry out the crosslinking or imidization reactions, depending on the chemistry. As the film is cooled, stresses are generated in the film due to a mismatch in the coefficient of thermal expansion (CTE) between the film and the substrate.<sup>3–6</sup> This, along with solvent evaporation-induced shrinkage, can cause the film to collapse in the through-plane direction, leading to molecular orientation in-the-plane of the film.<sup>7–9</sup> Such films tend to exhibit different electrical, thermal, and mechanical properties in-the-plane ( $x$ - $y$  or in-plane direction) versus normal-to-the-plane ( $z$  or through-plane direction) of the film.

Free-standing polymer films are commonly used in laminate and printed circuit board applications. Depending on the chemistry of the material and the processing history of the films, they may be isotropic or exhibit anisotropy, such as the orthotropic symmetry observed in films of Vectra, a thermotropic liquid crystalline polymer (LCP) (Hoechst Celanese). The orientation in this case

Correspondence to: P. A. Kohl (paul.kohl@che.gatech.edu).

\* Present address: IBM Corporation, Hopewell Junction, NY 12533.

*Journal of Applied Polymer Science*, Vol. 80, 2328–2334 (2001)  
© 2001 John Wiley & Sons, Inc.

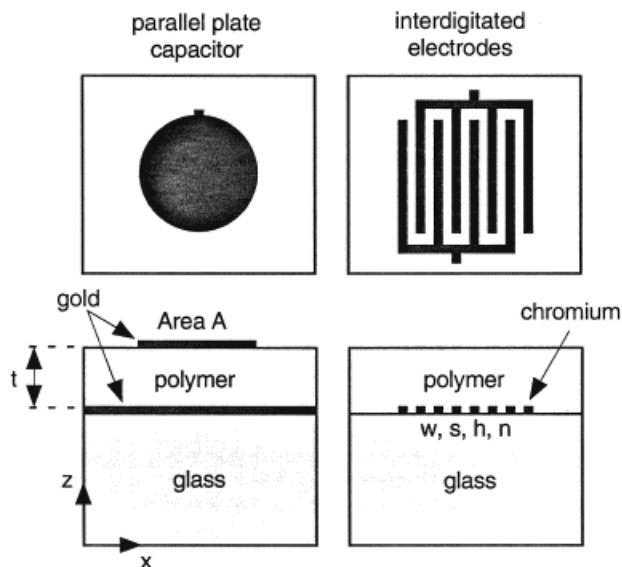


**Figure 1** Dual-capacitor device configuration for the anisotropic dielectric characterization of deposited polymer thin films.

results from spontaneous local arrangement of the polymer chains in the melt phase. Upon solidification, this orientation remains, and the resultant material exhibits anisotropy in properties.

This article presents the use of the dual-capacitor technique for measuring *in situ* the anisotropic dielectric permittivities of several spin-coated film as well as the first ever measurements of the orthotropic permittivities of free-standing Vectra films.

## THEORY

The principle behind the dual-capacitor technique is to model the capacitance of two devices, a parallel plate capacitor (PPC) and an interdigitated electrode (IDE) shown in Figure 1, which depends upon the anisotropic permittivities of the dielectric, and compare them with the experimentally measured values to determine the dielectric properties. This concept was employed by Lin<sup>7</sup> to study the molecular anisotropy of thin polymer films through dielectric characterization and later used by Weinberg<sup>10</sup> to characterize several common dielectric polymers. Variation of this approach, using serpentine instead of interdigitated electrodes, have also been reported.<sup>11,12</sup>

In order to model the response of the PPC, the expression for the capacitance between two un-

equal circular metal parallel plates separated by a dielectric was used:

$$C_{\text{PPC}} = \frac{\epsilon'_z \epsilon_0 A}{t} + C_f \quad (1)$$

where  $\epsilon'_z$  is the through-plane dielectric permittivity of the polymer,  $A$  is the area of the smaller capacitor plate,  $t$  is the thickness of the film,  $\epsilon_0$  is the permittivity of vacuum equal to  $8.854 \times 10^{-12}$  F/m, and  $C_f$  is the fringing field correction, which is insignificant if the diameter of the smaller capacitor plate is large compared with the film thickness  $t$ .<sup>13</sup>  $C_f$  was evaluated by modeling the capacitors using Maxwell EM 2D electromagnetic field simulator from Ansoft Corporation.

Because the PPC cannot be used to measure the in-plane dielectric permittivity, an interdigitated electrode (IDE) device was used. The response of the IDE structure was also modeled using Maxwell EM 2D. The two-dimensional electrostatic finite element model for a segment of the structure is shown in Figure 2. The model represents halves of two electrode digits viewed in cross section, with symmetric boundary conditions at the edges to take advantage of the periodicity in the interdigitated structure. The geometry variables shown in Figure 2 are  $w$ , the width of the electrode digit;  $s$ , the spacing between the digits;  $h$ , the thickness of the metal; and  $t$ , the thickness of the polymer film coating the elec-

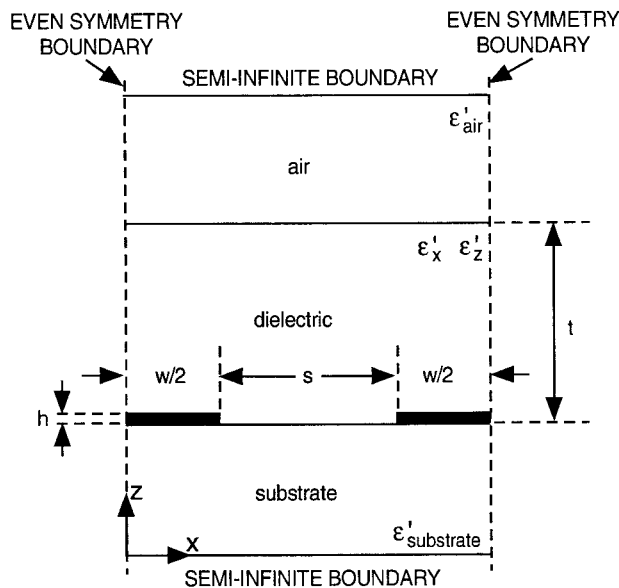


**Figure 2** Geometry for two-dimensional interdigitated electrode model.

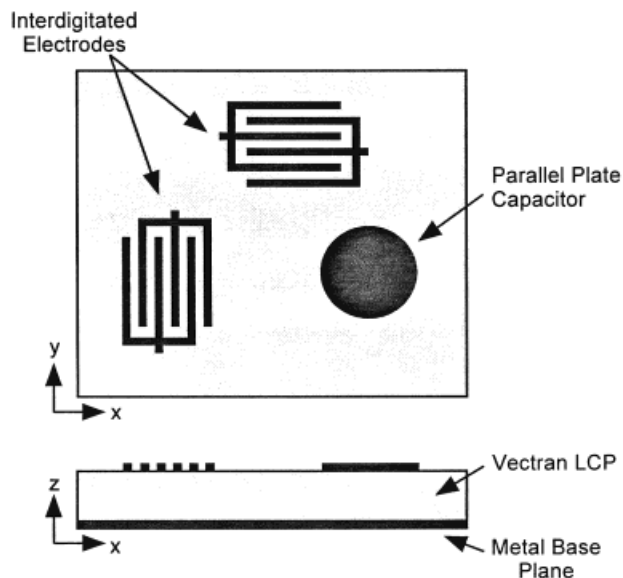


**Figure 3** Parallel plate capacitor and interdigitated electrode layout for the orthotropic dielectric characterization of free-standing Vectran films.

trode. Other inputs include: dielectric parameters  $\epsilon'_x$  or  $\epsilon'_y$ ,  $\epsilon'_z$ ,  $\epsilon'_{\text{air}}$ , and  $\epsilon'_{\text{substrate}}$ , which are the in-plane and through-plane permittivities of the polymer, the permittivities of air and the substrate respectively;  $n$ , the number of digits on each electrode, and  $l$ , the length of overlap between digits. In solving the model, a finite element mesh generated using a Delaunay triangulation algorithm was used. The mesh was adaptively refined until the change in total energy of the model was less than 0.01%.

In the case of free-standing films, the devices were fabricated directly onto the film, as shown in Figure 3. Electrodes with digits parallel to the  $x$ -direction allowed estimation of the permittivity along the  $y$ -direction since its fringing electric field remained in the  $y$ - $z$  plane. Similarly, IDE with digits along the  $y$ -direction helped attain permittivity along the  $x$ -direction. The finite element model used for simulating these electrodes was slightly different from the model shown in Figure 2, as there was no substrate. The base plane was not grounded during simulations, but its potential was allowed to float freely. Measurement of the capacitance and conductance between the electrodes were also made under similar conditions. Correction for fringing fields was important for the PPC devices because of the significant thickness-to-diameter ( $t:d$ ) ratio.

## EXPERIMENTAL

### Materials

The spin-coated polymer films examined in this work were benzocyclobutene (BCB)-based Cyclotene<sup>®</sup> 3022 and Cyclotene<sup>®</sup> 4026 (Dow Chemical Company); polynorbornene (PNB)-based Avatrel<sup>®</sup> (BF Goodrich); and polyimide PI-2611 [biphenyldianhydride (BPDA)]; and  $p$ -phenylenediamine (PDA) (HD MicroSystems). Cyclotene<sup>®</sup> 4026 is a photosensitive version of BCB. The BCB- and PNB-based polymers were selected because they were likely to be isotropic, whereas the polyimide PI-2611 is known to be highly anisotropic because of its rigid-rod nature. The chemical structures of the monomers of these polymers are shown in Figure 4, along with monomers for polyimide PI-2540 [pyromellitic dianhydride (PMDA)] and 4,4'-oxydianiline (ODA) (HD MicroSystems) and preimidized polyimide Probimide 293 [benzophenone-3,3', 4,4'-tetracarboxydianhydride (BTDA)] and trimethyldiaminophenylindane (DAPI) (OCG

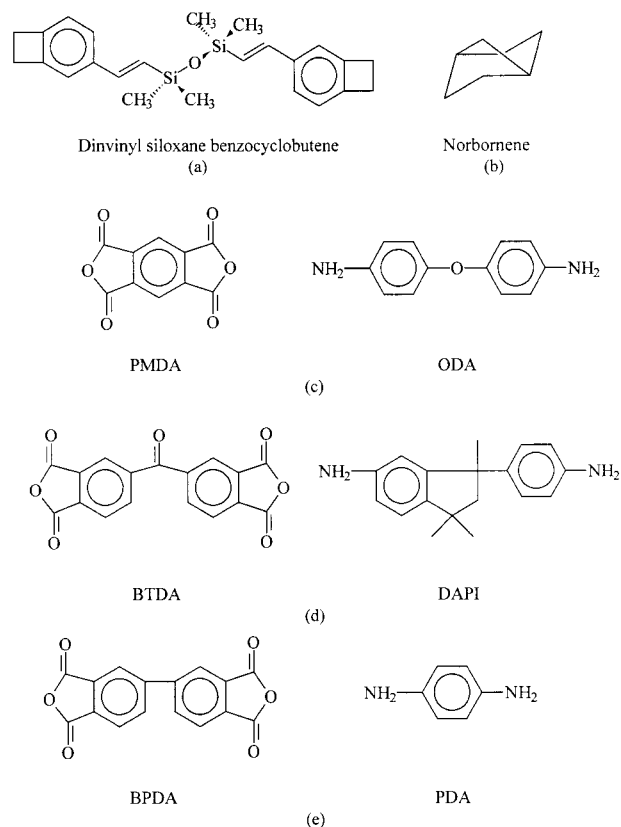


**Figure 4** Chemical monomeric units for (a) Cyclotene 3022 and 4026, (b) Avatrel, (c) PI-2540, (d) Probimide 293, and (e) PI-2611.

Microelectronics). PI-2540 and Probimide 293 were characterized by Weinberg,<sup>10</sup> using a similar technique but with a slightly different approach with regard to device configuration and fabrication.

In addition to the solvent cast-deposited films, free-standing films of Vectra (2-naphthalenecarboxylic acid, 6-(acetyloxy)-, polymer with 4-(acetoxy)benzoic acid), a thermotropic liquid crystalline polymer (LCP) from Hoechst Celanese, were also evaluated. These films are available commercially as copper-clad laminate films under the brand name Vectran for use in printed circuit board and laminated multichip module (MCM-L) applications; these films reportedly offer several favorable properties, such as low through-plane (*z*) dielectric constant (3.1 at 1 MHz), low moisture absorption, chemical resistance, and compatibility with current processes.<sup>14</sup> The laminate consisted of a 95–120- $\mu\text{m}$ -thick LCP film sandwiched between two layers of 25- $\mu\text{m}$ -thick electrodeposited copper. A glass-reinforced version, containing a fiberglass fabric within the LCP for additional reinforcement, is available and was also evaluated in this study. These films differed from the spin-coated films in that their properties were not axisymmetric. Thus, the films were characterized assuming orthotropic symmetry with the principal directions corresponding with the directions in which the film was drawn during processing, as indicated by the manufacturer.

### Devices

To characterize the spin-coated films, parallel plate capacitors and interdigitated electrodes were fabricated with the polymer as the dielectric and low-expansion borosilicate glass, with a dielectric permittivity of 7.3, as the substrate. The PPC were fabricated by first sputtering the glass with a thin adhesion layer of titanium and 3000 Å of gold. The metal surface was then treated with an adhesion promoter and spin-coated with polymer to obtain films of 8–12- $\mu\text{m}$  thickness. The adhesion promoter used for BCB and PI-2611 was 3-aminopropyltriethoxysilane and HD MicroSystems adhesion promoter VM 651, respectively, no adhesion promoter was required for Avatrel. The polymer was then cured for 1 h at 250°C for Cyclotene 3022 and 4026, 350°C for PI-2611, and 300°C for Avatrel, to obtain the dielectric film. Cyclotene 4026, which is a negative tone photopolymer, required an extra ultraviolet (UV) exposure step before the final cure, to ensure

crosslinking. The films were flood-exposed at a dose higher than the 750–900 mJ/cm<sup>2</sup> to ensure complete crosslinking, followed by soaking in the Dow developer DS-2100 for 2 min to remove all unreacted photoadditives. Once the films were cured, a thin titanium adhesion layer and 3000 Å of gold was sputtered onto the polymer and patterned using photolithography to form 10-mm-diameter circular capacitors.

The interdigitated electrodes were fabricated from chromium coated glass plates by a mask making procedure involving photolithography. The glass mask plates, coated with 3000 Å of chromium and 5600 Å of Shipley 1805 photoresist, and without the antireflective coatings of chromium oxide and chromium nitride, were obtained from Telic Corporation (Santa Clara, CA). First, a mask design with the IDE pattern magnified  $\times 10$  was created and transferred onto an emulsion plate, using a mask generator. The emulsion plate was then used as a mask to project the design onto the photoresist-coated chromium mask plates using a  $\times 10$  reduction UV stepper. After the resist was developed and baked, the chromium was etched to form the electrodes. Finally, the dimensions of the IDE were measured and the devices coated with the polymer film. The capacitance of the IDE was measured by probing the device through this film.

In the case of Vectran, interdigitated electrodes and parallel plate capacitors were fabricated directly onto the films, which were rigid enough for the devices to survive processing. Vectran was received as a copper-clad sheet with 25  $\mu\text{m}$  of copper on both sides. Care was taken to mark the principal directions on the test sections, consistent with the marking made by the manufacturer. The copper on one side of the sheet was etched away in dilute sulfuric acid, while protecting the other side with a protect coat of Shipley SC 1827 photoresist. A 3500-Å-thick layer of gold with a thin adhesion layer of titanium was then sputtered onto the exposed side using DC sputtering. The reason for replacing the top layer was to avoid problems associated with fabricating the electrodes from the original 25- $\mu\text{m}$ -thick copper layer. The purpose of the bottom metal layer was to provide additional rigidity to the film and prevent it from bending or warping during etch due to stress imbalance in the LCP. The gold layer was patterned using photolithography to form circular capacitors and interdigitated electrodes. The devices were ready for testing, once the photoresist layers were stripped away in acetone. The

**Table I** Dimensions of Interdigitated Electrodes and Parallel Plate Capacitors Used to Characterize Deposited and Free-Standing Films

	Spin-Coated Dielectric Films	Free-Standing Vectran Films
Thickness of the dielectric	8–12 $\mu\text{m}$	97 $\mu\text{m}$ (nonreinforced) 116 $\mu\text{m}$ (glass-reinforced)
Parallel plate capacitor		
Diameter, $d$	10 mm	12 mm
Interdigitated electrodes		
Width, $w$	3 $\mu\text{m}$	60 $\mu\text{m}$
Spacing, $s$	3 $\mu\text{m}$	40 $\mu\text{m}$
Number of digits, $n$	200	50
Overlap of digits	6.8 mm	9.5 mm
Total meander length	2.7132 m	0.9405 m

dimensions of the PPC and IDE devices used for characterizing deposited and free-standing films are listed in Table I. The depth of the polymer sampled for the IDE device (depth of penetration) was greater than the spacing between the electrodes (and falls off with distance from the electrode). The IDE had a spacing of 40  $\mu\text{m}$  (Table I) and the thickness of the nonreinforced and glass-reinforced Vectran was 97 and 116  $\mu\text{m}$ , respectively. Thus, the IDE sampled much of the thickness of each film.

Before testing, the critical dimensions of the fabricated devices and the thickness of the spin-coated films were measured using an Alphastep Profilometer. The thickness of the Vectran sheet was measured at several points close to the devices, using a thickness gauge, and averaged. The capacitance of the devices was then measured using a Hewlett-Packard 4263A LCR meter at a test frequency of 10 kHz.

## RESULTS AND DISCUSSION

The chemical structures of the monomers used to form the polymers reported in this study are shown in Figure 4. The direction-dependent dielectric properties for several materials were measured and compared with properties for two polymers, HD Microsystems Polyimide PI-2540 and pre-imidized OCG Microelectronics Probimide 293, as previously reported.<sup>10</sup> The first objective of this study was to validate the experimental and modeling approach for measurement of direction-dependant permittivities. For this purpose, the spin-coated materials shown in Table IIA were measured or obtained from earlier litera-

ture.<sup>10</sup> Cyclotene 3022 and 4026 are isotropic, thermosetting polymers, and PI 2611, PI 2540 and Probimide 293 are thermoplastic polyimides.

Figure 5 plots the in-plane ( $x$ - and  $y$ -direction) permittivity as a function of the through-plane ( $z$ ) permittivity. The polymers listed in Table IIA were spin-coated; they have identical properties in the  $x$  and  $y$  (in-plane) directions. Thus, there is only one value of permittivity reported on the abscissa of Figure 5 for the polymers in Table IIA because  $\epsilon'_x = \epsilon'_y$ . Those polymers straddling the 45-degree line in Figure 5 have isotropic behavior for in-plane ( $\epsilon'_x$  or  $\epsilon'_y$ ) and through-plane properties ( $\epsilon'_z$ ),  $\epsilon'_x = \epsilon'_y = \epsilon'_z$ . Points that lie off the 45-degree line exhibit in-plane versus through-plane anisotropy with  $\epsilon'_x$  not equal to  $\epsilon'_z$ . Three of the spin-coated materials in Figure 5 and Table IIA (i.e., Probimide 293, PI-2611, and PI-2540) have in-plane permittivities greater their through-plane permittivity. This results from orientation of the polymer during processing and curing.

The second objective of this study was to examine materials in which the in-plane permittivities ( $x$ - and  $y$ -directions) were not the same. For this, the orthotropic permittivities of two types of Vectran film were measured. The data are plotted in Figure 5 and listed in Table IIB. Two in-plane permittivity values ( $\epsilon'_x$  and  $\epsilon'_y$ ) are plotted in Figure 5 for the reinforced and nonreinforced Vectran. The loss tangent  $\tan \delta_z$  equal to  $G/2\pi fC$ , where  $G$  is the conductance,  $C$  is the capacitance of the PPC, and  $f$  is the frequency of measurement (10 kHz), calculated to be 0.0324 and 0.0299 for the nonreinforced and glass-reinforced films, respectively. The nonreinforced and glass-reinforced films show a large anisotropy with a higher permittivity for the through-plane compared with

**Table II** Summary of Measured Dielectric Permittivities

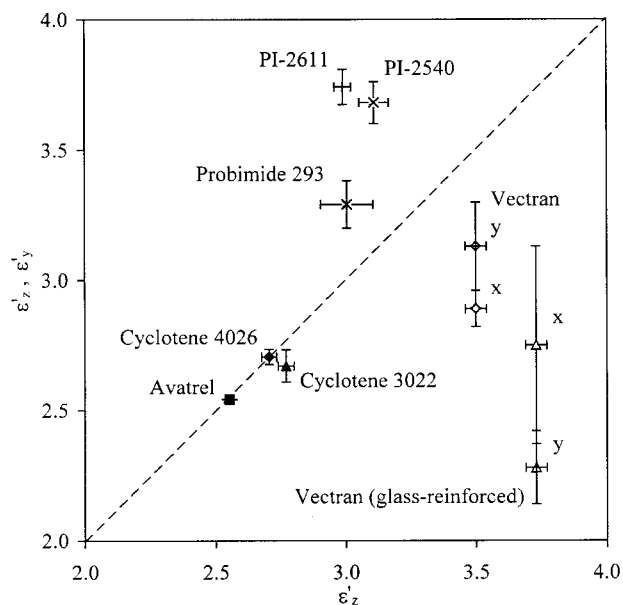
A. Spin-Coated Films			
Polymer	$\epsilon'_z$	$\epsilon'_z = \epsilon'_y$	
Cyclotene® 3022	$2.77 \pm 0.03$	$2.67 \pm 0.06$	
Cyclotene® 4026	$2.71 \pm 0.03$	$2.71 \pm 0.03$	
Avatrel®	$2.55 \pm 0.03$	2.54	
PI-2611 (BPDA/PDA)	$2.99 \pm 0.03$	$3.74 \pm 0.07$	
PI-2540 (PMDA/ODA) [10]	$3.11 \pm 0.06$	$3.68 \pm 0.08$	
Probimide 293 (BTDA/DAPI) [10]	$3.01 \pm 0.10$	$3.29 \pm 0.09$	

B. Free-Standing Vectran Films				
Vectran®	$\epsilon'_z$	$\tan \delta_z$	$\epsilon'_x$	$\epsilon'_y$
Nonreinforced	$3.50 \pm 0.04$	$0.032 \pm 0.001$	$2.89 \pm 0.07$	$3.13 \pm 0.17$
Glass-reinforced	$3.73 \pm 0.04$	$0.030 \pm 0.001$	$2.75 \pm 0.38$	$2.28 \pm 0.14$

the in-plane directions. The  $x$ - and  $y$ -directions for the reinforced and nonreinforced Vectran were identified with respect to the direction that the films were extruded. The degree of anisotropy for the glass-reinforced film in the  $y$ -direction ( $\epsilon'_y$ ) is lower than in the  $x$ -direction ( $\epsilon'_x$ ), whereas for the nonreinforced case, the results show the opposite trend. These results are reproducible and appear to reflect differences in processing and degree of orientation induced by the presence of the glass-

reinforcement. The properties of the glass fibers, presence of voids, and polymer orientation due to the presence of the fibers were not investigated. The anisotropy in the polymer chains is due to crystallization of the LCP along the direction of draw during processing. Because the modulus along the chains is much greater than the modulus normal to it, the LCP films have exceptional mechanical properties along the direction of draw, but they are moderate otherwise. The glass fiber reinforcement is used to improve their overall mechanical robustness of the film. A direct quantitative comparison of the reinforced with the nonreinforced Vectran is not possible because of processing differences attributable to the presence of the fiber. During processing, the LCP sheets form distinct skin and core regions, which may cause different degrees of anisotropy due to the presence of the filler.<sup>15,16</sup> Since the individual properties of the fiber and effect of the fiber on the packing of the LCP (around the fiber) were not investigated, the origin of the differences in  $\epsilon'_x$  and  $\epsilon'_y$  between the nonreinforced and glass-reinforced fiber cannot be identified with certainty. Any changes in the void fraction of the polymer or packing of the LCP (due to the presence of the fiber) could have a significant effect on the dielectric constant. The skin region is typically highly oriented due to the larger shear forces during processing and hence may exhibit greater anisotropy than the core. The presence of the fiber changes the film fabrication process and the electric field distribution during the measurements



**Figure 5** Plot of the anisotropic dielectric permittivities of spin-coated polymer films and free-standing Vectran films characterized in this study.

because the two materials have different dielectric properties.

Care was taken to orient the in-plane electrodes both parallel and perpendicular to the direction of laminate extrusion. If another set of normal directions within the plane of the LCP sheet were to be selected instead, for example at 45 degrees to the edge of the sheet, the permittivity results and the observed anisotropy would be different. These cannot be estimated by coordinate transformation of the reported results unless the off-diagonal terms in the dielectric permittivity tensor are first determined, and hence would have to be remeasured. This is a characteristic of all orthotropic materials; mechanical properties, such as modulus and tensile strength, have been shown to follow this trend for other Vectra-based LCP.<sup>15</sup> This may explain the higher standard deviations observed for in-plane measurement, as ensuring perfect alignment was not always possible.

## CONCLUSIONS

The use of the dual-capacitor technique to measure the anisotropic dielectric permittivities of spin-cast and free-standing polymer films was demonstrated. In this technique, two devices—an interdigitated electrode and a parallel plate capacitor—were fabricated with the polymer as the dielectric and their capacitance is measured. The devices were then modeled using an electrostatic finite element model and the results compared with the experimentally measured values to determine the directional permittivities. Results were reported for spin-on dielectrics Cyclotene 3022, Cyclotene 4026, Avatrel, and PI-2611. With the exception of polyimide PI-2611, which showed a large anisotropy between its in-plane and through-plane permittivities, the remaining polymers were isotropic in nature. Also reported for the first time was the orthotropic characterization of free-standing Vectran LCP films, including a glass-reinforced version. The films displayed large anisotropy and a through-plane permittivity that was much higher than its in-plane value. The glass-reinforced film showed larger anisot-

ropy, lower overall permittivity, and greater inhomogeneity than the did the nonreinforced film due to the presence of the embedded glass fabric. The measured values were also found to be highly dependent on the selected set of orthogonal directions, orientation of the glass fabric, and the large-scale order and morphology of the LCP matrix.

## REFERENCES

1. Tummala, R. R.; Ryamaszewski, E. J., Ed. *Microelectronics Packaging Handbook*. Van Nostrand-Reinhold: New York, 1997.
2. Garrou, P. *Proc IEEE* 1992, 80, 1942.
3. Tong, H. M.; Hu, C.-K.; Feger, C.; Ho, P. S. *Polym Eng Sci* 1986, 26, 1213.
4. Bauer, C. L.; Farris, R. J. In *Polyimides: Materials, Chemistry and Characterization*; C. Feger, Khojasteh, M. M.; McGrath, J. E., Eds.; Elsevier: Amsterdam, 1989; p 549.
5. Pottiger, M. T.; Coburn, J. *Mater Res Soc Symp Proc* 1991, 227, 187.
6. Coburn, J. C.; Pottiger, M. T.; Noe, S. C.; Senturia, S. D. *J Polym Sci Polym Phys* 1994, 32, 1271.
7. Lin, L., Ph.D. Dissertation, Georgia Institute of Technology, Atlanta, GA, 1994.
8. Molis, S. E. In *Polyimides: Materials, Chemistry and Characterization*; Feger, C.; Khojasteh, M. M.; McGrath, J. E. Eds.; Elsevier: Amsterdam, 1989; p 659.
9. Boese, D.; Lee, H.; Yoon, D. Y.; Swalen, J. D.; Rabolt, J. F. *J Polym Sci Polym Phys* 1992, 30, 1321.
10. Weinberg, S. Masters thesis, Georgia Institute of Technology, Atlanta, GA, 1996.
11. Ryan, E. T.; Cho, T.; Malik, I.; Zhao, Z.-H.; Lee, J. K.; Ho, P. S. *Mater Res Soc Symp Proc* 1997, 476, 135.
12. Loke, A. L. S.; Wetzel, J. T.; Stankus, J. J.; Wong, S. S. *Mater Res Soc Symp Proc* 1997, 476, 129.
13. Clausius, R. *Die Mechanische Wärmetheorie; Vol II*; Braunschweig, 1879.
14. Culbertson, E. C. Presented at the Proceedings of the 45th ECTC, 1995; p 520.
15. Plummer, C. J. G.; Wu, Y.; Davies, P.; Zulle, B.; Demarmels, A.; Kausch, H.-H. *J Appl Polym Sci* 1993, 48, 731.
16. Jansen, J. A. J.; Paridaans, F. N.; Heyndericks, I. E. *J Polymer* 1994, 35, 2970.